Supporting Information

Mason et al. 10.1073/pnas.1215097110

SI Materials and Methods

Mice and Hematopoietic Reconstitution. All experiments with mice were performed according to the guidelines of the Animal Ethics Committee of the Walter an Eliza Hall Institute of Medical Research (WEHI). The *bak*$^{-/-}$ (1) and *bax*$^{-/-}$ mice (2), both originally on a mixed C57BL/6 × 129SV background (produced from 129SV-derived ES cells), were backcrossed for >10 generations onto a C57BL/6 background at WEHI and were only then intercrossed to generate *bak*$^{-/-}$*bax*$^{+/-}$ mice. These animals were then intercrossed to produce Bak/Bax doubly deficient animals. Embryonic day (E)13.5 embryos were harvested from intercrosses of *bak*$^{-/-}$*bax*$^{+/-}$ mice and fetal liver cells (FLC) suspensions prepared to reconstitute the hematopoietic compartment of lethally irradiated (2 × 5.5 Gy, 2 h apart) C57BL/6-Ly5.1 mice (2 × 10^6 FLC injected i.v. per recipient). DNA extracted from tails of embryos was prepared for genotyping for *bax* to select for FLC of the appropriate genotype for hematopoietic reconstitution. At 8–10 wk after reconstitution, peripheral blood leukocytes were stained for Ly5.1 and Ly5.2 to assess the extent of hematopoietic reconstitution by donor-derived (Ly5.2) cells, which consistently was >95%. The *vav-BCL-2* transgenic mice (generated on an inbred C57BL/6-Ly5.2 background) have been previously described (3). Mice were monitored daily for morbidity and killed when showing signs of illness. Urine analysis was performed using Multistix 10SG (Siemens). Blood was analyzed in an Advia 2120 hematology system (Siemens).

Histological Analysis. Tissues were fixed for microscopic analysis in 80% (vol/vol) Histochoice (Amresco)/20% (vol/vol) methanol and embedded in paraffin, and conventional histopathology was performed on H&E-stained sections. H&E-stained sections of kidneys from mice were examined for evidence of glomerulonephritis (GN) and scored on a scale of 0–4: 0 = normal, 1 = minor mesangial hypercellularity, 2 = moderate hypercellularity with obliteration of capillary loops, 3 = severe hypercellularity with obliteration and thickening of all capillary loops, 4 = 3 plus fibrinoid necrosis. Lymphoid infiltrates into organs (lung, liver, kidney, pancreas, submandibular gland) were assessed on H&E-stained sections and graded 0–3: 0 = none, 1 = occasional small, perivascular foci (age related), 2 = more dense, well-defined perivascular and periductal foci, 3 = extensive infiltrate with parenchymal destruction. H&E-stained spleen sections were graded 0–4: 0 = normal, 1 = absent germinal center and expansion of perifollicular zone, 2 = 1 plus expansion of interfollicular plasma cells, 3 = 2 plus follicular dendritic cell expansion, 4 = 3 plus necrotizing vasculitis. H&E-stained lymph node sections were scored 0–3: 0 = normal, 1 = paracortical T-cell expansion with none or reduced B-cell follicles (dematopathic changes), 2 = 1 plus increased medullary plasma cells, 3 = 2 plus expansion of interdigitating reticulum cells. H&E-stained thymus sections were graded 0–1: 0 = normal, 1 = absence of medulla. All tissue sections were assessed in a blinded manner by a qualified pathologist (P.W.). All photomicrographs were acquired using a 10×/N.A. 0.3, 20×/N.A. 0.50, or 40×/N.A. 0.75 objective lens attached to an Axioplan 2 microscope (Carl Zeiss MicroImaging).

Flow Cytometric Analysis, Immunofluorescent Staining, and Confocal Microscopy. Single-cell suspensions of spleen, lymph nodes (pooled axillary, brachial, inguinal, mesenteric), and peripheral blood were stained as previously described (4) using FITC- or R-Phycoerythrin (R-PE)-conjugated surface marker-specific mAbs (RB6-8C5: anti-Gr-1; MI/70: anti-Mac-1; M3/84.6.34: anti-Mac-2; Ter119: anti-erythroid cell surface marker; F4/80: anti-macrophage surface marker; T24.31.2: anti-Thy-1; GK1.5: anti-CD4; 53.6.72: anti-CD8; RA3-6B2: anti-CD45R-B220; PK136: anti-NK1.1) (BD Biosciences). T regulatory cells were detected by surface staining with R-PE anti-CD25, FITC anti-CD4 and, after fixation and permeabilization, with APC anti-FoxP3 antibodies, according to the manufacturer's instructions (eBiosciences). Plasma cells were detected by staining with antibodies to B220 (R-PE conjugated) and CD138$^+$ (FITC conjugated), and B10 regulatory B cells were revealed with antibodies to CD19 (FITC conjugated), CD5 (R-PE conjugated), and CD1d$^+$ (biotinylated) using secondary staining with avidin-PE-Cy-7 (all from BD Pharmingen). The vital dye propidium iodide (PI) (1 μg/mL) was used to exclude dead cells (except for cells that were also stained intracellularly) and cells analyzed in a FACScan (Becton Dickinson). Surface FasL expression was detected according to ref. 4.

To stain for immune complex deposits, kidney cryo-sections (5 μm) were acetone fixed and blocked with PBS/2% (vol/vol) FCS, followed by staining with FITC-coupled goat antibodies specific to mouse IgM, IgG, or IgA (Southern Biotechnology) in PBS/2% (vol/vol) FCS with DAPI (to stain nuclei), as previously described (4). Antinuclear autoantibodies (ANA) in sera of mice were detected by immunofluorescent staining of slides coated with HEp2 human epithelial cells (4) and semiquantified according to brightness of fluorescence intensity on a scale of 0 (no fluorescence) to 3+ (maximum fluorescence intensity) as previously described (4). For serum analysis of anti-neutrophil cytoplasmic autoantibodies (ANCA), sera from hematopoietically reconstituted mice were diluted 1/20 and then used for staining of slides containing ethanol-fixed human neutrophils (NOVA Lite; INOVA Diagnostics). Bound antibodies were detected by secondary staining with FITC-conjugated antibodies to mouse IgG (Pharmingen). Slides were scored by an experienced hospital diagnostic laboratory technician and then reexamined by a clinical specialist and scored according to type: cytoplasmic (c-ANCA), perinuclear (p-ANCA), atypical ANCA, and granulocytic, all semiquantified according to brightness of fluorescence intensity on a scale of 0 (no fluorescence) to 4+ (maximum fluorescence intensity). As a positive control, we used sera from C57BL/6$^{gld/gld}$ mice, which had been shown to have ANA.

For confocal microscopic detection of organ-specific autoantibodies in sera of sick mice, 5-μm frozen sections of eye, ovary, salivary gland, stomach, pancreas, liver, lung, prostate, thyroid/parathyroid glands, and kidney from 8-wk old *rag-1*$^{-/-}$*/J* mice (to avoid endogenous Ig in the tissues) were incubated with 1/100 dilutions of sera from test mice and secondarily stained with FITC-conjugated goat antibodies specific for mouse IgG, IgM, and IgA (Cappel, MP Biomedicals) plus DAPI (Sigma) as previously described (5) and visualized on a Leica DIMIRE2 confocal microscope (Leica Microsystems).

ELISA. Serum Ig concentrations were measured by ELISA as previously described (6). Purified myeloma proteins (at known concentrations) were used as standards (Sigma). ANA levels were also measured by ELISA by using the Bindazyme ANA Kit (Binding Site) according to the manufacturer's instructions.

Measurement of Serum Cytokine and Chemokine Levels. Cytokine and chemokine concentrations in sera of mice were measured by

using the Bio-Plex Pro mouse cytokine 23-plex immunoassay (Bio-Rad) following the manufacturer's instructions.

Western Blotting. Cell lysates were prepared in radioimmunoprecipitation assay lysis buffer and proteins size-fractionated on polyacrylamide gels (Novex) and transferred to nitrocellulose membranes (Amersham Pharmacia) as previously described (4). Membranes were then probed with the following antibodies: rabbit anti-Mcl-1 (Rockland) and mouse anti-HSP70 mAb N6 (4), the latter to control for the concentration and integrity of proteins in the tissue lysates. Bound antibodies were visualized with sheep anti-rabbit Ig (Chemicon) or sheep anti-mouse IgG antibodies (Chemicon), both conjugated to HRP, followed by enhanced chemiluminescence (ECL; Amersham Pharmacia).

Cell Death Analysis. Apoptotic and necrotic cells in cultures of lymph node cells were identified by flow cytometric analysis (FACScan; Becton-Dickinson) after staining with PI and FITC-conjugated Annexin V. PI^{-}FITC-Annexin V^{+} cells were considered to be early apoptotic, PI^{+}FITC-Annexin V^{+} cells were considered to be late apoptotic, whereas PI^{+}FITC-Annexin V^{-} cells were considered to be necrotic.

Statistical Analysis. For comparison of animal survival curves and GN incidence, the log–rank (Mantel-Cox) test was used. For comparison of organ weights, serum Ig levels, lymphocyte numbers, platelet counts, GN index, ANA ELISA, and grade of Ig deposition, the unpaired Student *t* test was used ($^{*}P < 0.05$, $^{**}P < 0.005$, $^{***}P < 0.005$).

1. Lindsten T, et al. (2000) The combined functions of proapoptotic Bcl-2 family members bak and bax are essential for normal development of multiple tissues. *Mol Cell* 6(6): 1389–1399.
2. Knudson CM, Tung KSK, Tourtellotte WG, Brown GAJ, Korsmeyer SJ (1995) Bax-deficient mice with lymphoid hyperplasia and male germ cell death. *Science* 270(5233):96–99.
3. Ogilvy S, et al. (1999) Constitutive Bcl-2 expression throughout the hematopoietic compartment affects multiple lineages and enhances progenitor cell survival. *Proc Natl Acad Sci USA* 96(26):14943–14948.
4. O' Reilly LA, et al. (2009) Membrane-bound Fas ligand only is essential for Fas-induced apoptosis. *Nature* 461(7264):659–663.
5. Jiang W, Anderson MS, Bronson R, Mathis D, Benoist C (2005) Modifier loci condition autoimmunity provoked by Aire deficiency. *J Exp Med* 202(6):805–815.
6. Hibbs ML, et al. (1995) Multiple defects in the immune system of *Lyn*-deficient mice, culminating in autoimmune disease. *Cell* 83(2):301–311.

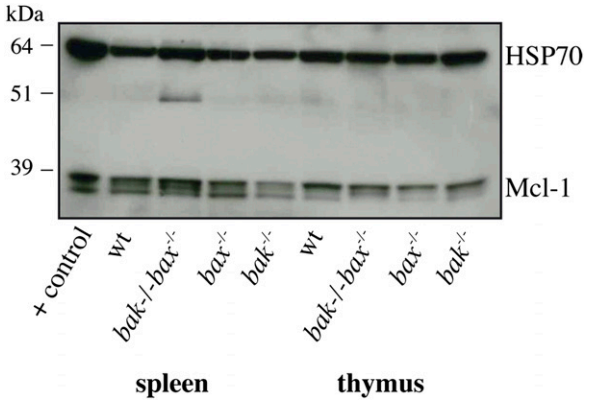

Fig. S1. Western blot analysis of Mcl-1 expression in spleen and thymus cells from Ly5.1 mice reconstituted with FLC of the indicated genotypes. Probing with an antibody to Hsp70 was used as a loading control.

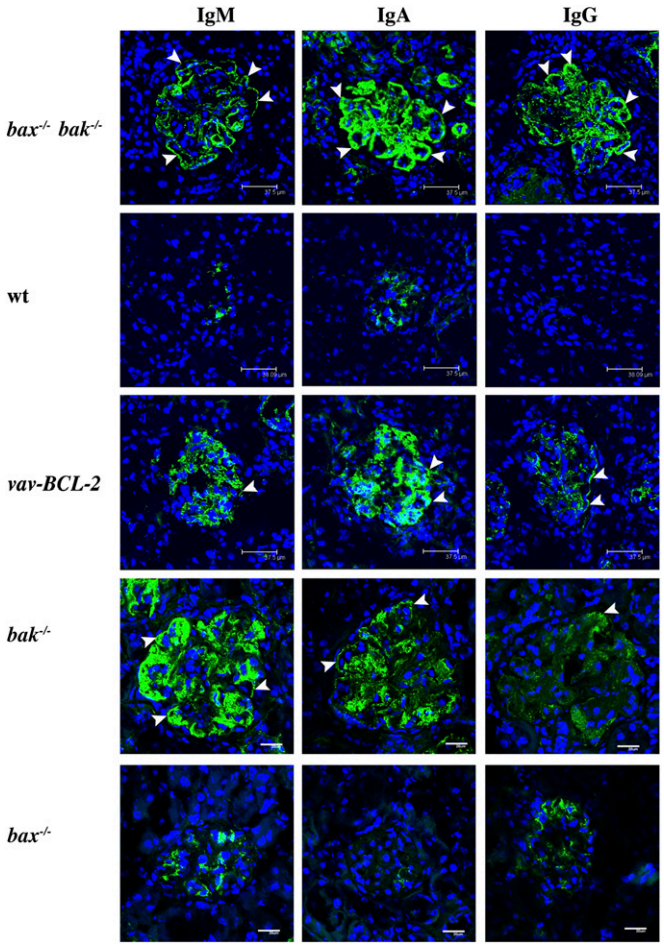

Fig. S2. Ig deposition in renal glomeruli of mice reconstituted with a $bak^{-/-}bax^{-/-}$ hematopoietic system. Representative photomicrographs of frozen sections (from 6 to 10 kidneys) of Ly5.1 mice reconstituted with FLC of the indicated genotypes stained for the presence of IgA-, IgG-, or IgM-containing immune complexes (green) in glomeruli. Nuclei are revealed by staining with DAPI (blue). Arrows indicate Ig deposition on the glomerular basement membrane. (Scale bars: 20 or 37.55 μm, as indicated.)

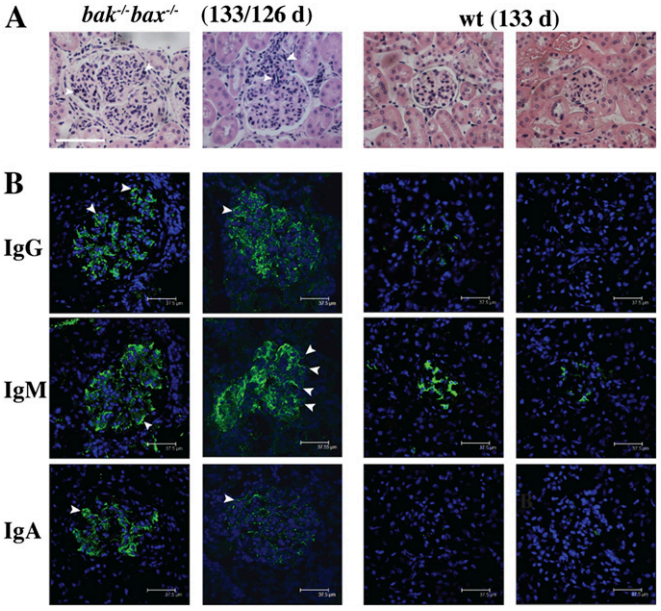

Fig. S3. The few $bak^{-/-}bax^{-/-}$ mice that survive to adulthood develop GN, lymphadenopathy, and splenomegaly. (*A*) Photomicrographs of H&E-stained sections of renal glomeruli from two of the four $bak^{-/-}bax^{-/-}$ mice that survived to early adulthood and, as a comparison, from two age-matched control WT mice. Arrows indicate infiltrating inflammatory cells. (*B*) Representative images of renal glomeruli from two of the four $bak^{-/-}bax^{-/-}$ mice that survived to early adulthood and those from two age-matched WT mice that were stained to reveal deposition of IgM, IgA, and IgG. Arrows indicate Ig deposition on the glomerular capillary loops.

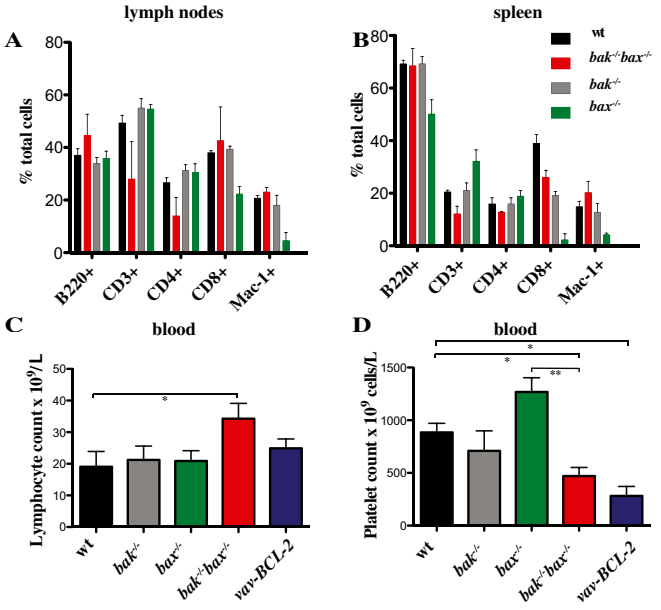

Fig. S4. Abnormal expansion of lymphoid and myeloid cell populations in secondary lymphoid organs coupled with lymphocytosis and thrombocytopenia in mice reconstituted with a $bak^{-/-}bax^{-/-}$ hematopoietic system. Percentages of lymphoid cell subpopulations in (*A*) lymph nodes and (*B*) spleens of Ly5.1 mice reconstituted with FLC of the indicated genotypes were determined by flow cytometric analysis. Lymphocyte counts were significantly elevated (*C*) and platelet counts significantly decreased (*D*) in peripheral blood of Ly5.1 mice reconstituted with $bak^{-/-}bax^{-/-}$ FLC cells compared with control mice reconstituted with WT FLC (*$P < 0.05$; **$P < 0.005$). Data represent mean ± SEM. Data were derived from sick mice that had to be killed ($bak^{-/-}bax^{-/-}$, $bak^{-/-}$, or *vav-BCL-2* reconstituted) or from mice at the end of the experiment ($bax^{-/-}$ or WT reconstituted).

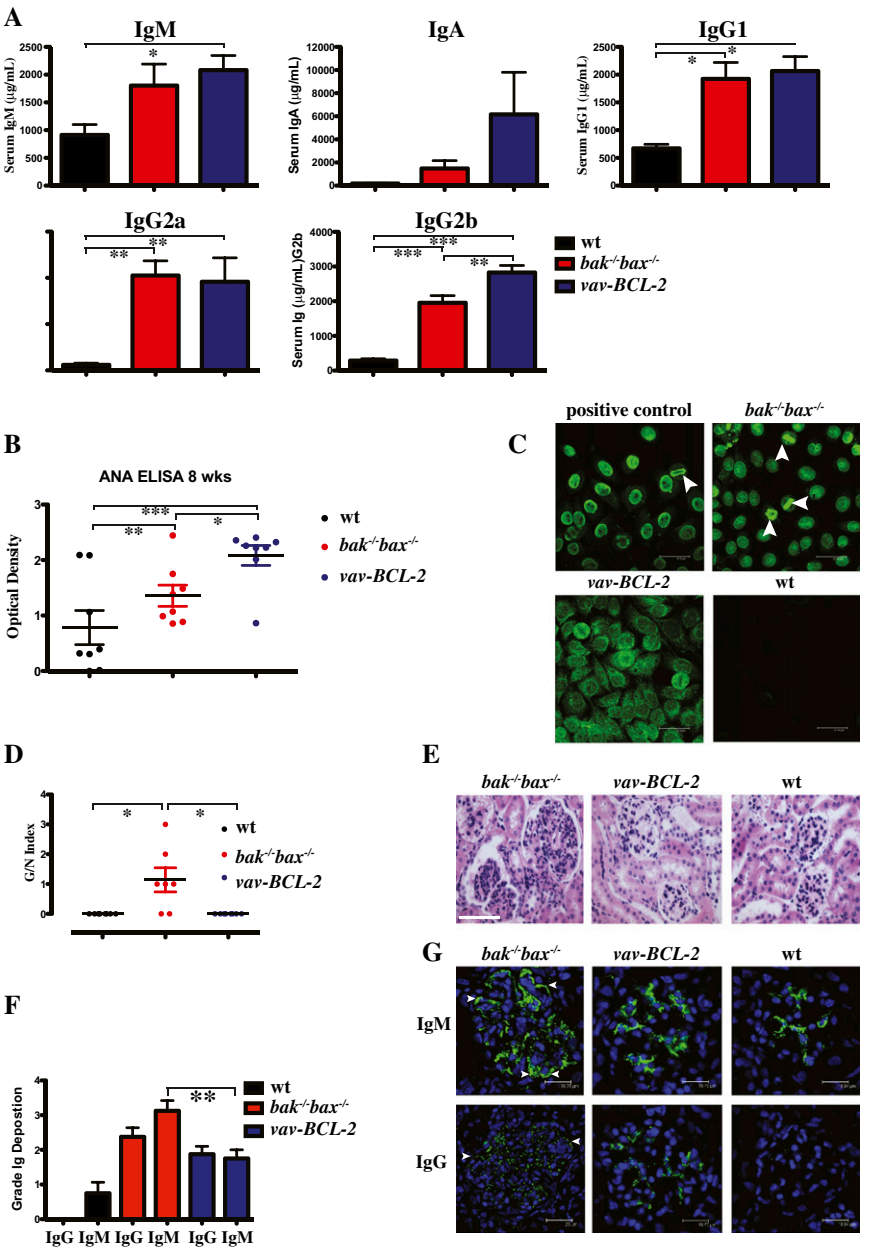

Fig. S5. Mice reconstituted with a *bak*$^{-/-}$*bax*$^{-/-}$ hematopietic system develop GN more rapidly than mice reconstituted with a *vav-BCL-2* hematopoietic system. (*A*) Ly5.1 mice reconstituted with *bak*$^{-/-}$*bax*$^{-/-}$, *vav-BCL-2*, or WT FLC were killed at 8 wk after reconstitution (n = 8 per genotype) and their sera analyzed by ELISA for the levels of IgM, IgA, IgG1, IgG2a, and IgG2b (*A*) and for the levels of ANA, either by ELISA (*B*) or immunofluorescence staining of slides covered with HEp2 cells (*C*). Arrows in *C* indicate staining of nuclear components in mitotic figures. Sections of kidneys of mice reconstituted with a hematopietic system of the indicated genotypes were graded for disease severity (*D*, scale 0–4), and representative photomicographs are shown (*E*). Data on IgM, IgA, and IgG deposition on the glomerular basement membrane (graded 0–4 according to staining) are summarized in *F* and illustrated by representative confocal micrographs in *G*. Arrows indicate Ig deposition on the glomerular basement membrane. Mean = SEM. *$P < 0.05$; **$P < 0.005$; ***$P < 0.0005$. (Scale bars: 37.5 μm in *C*, 128 μm in *E*, 8.75 μm in *G*.)

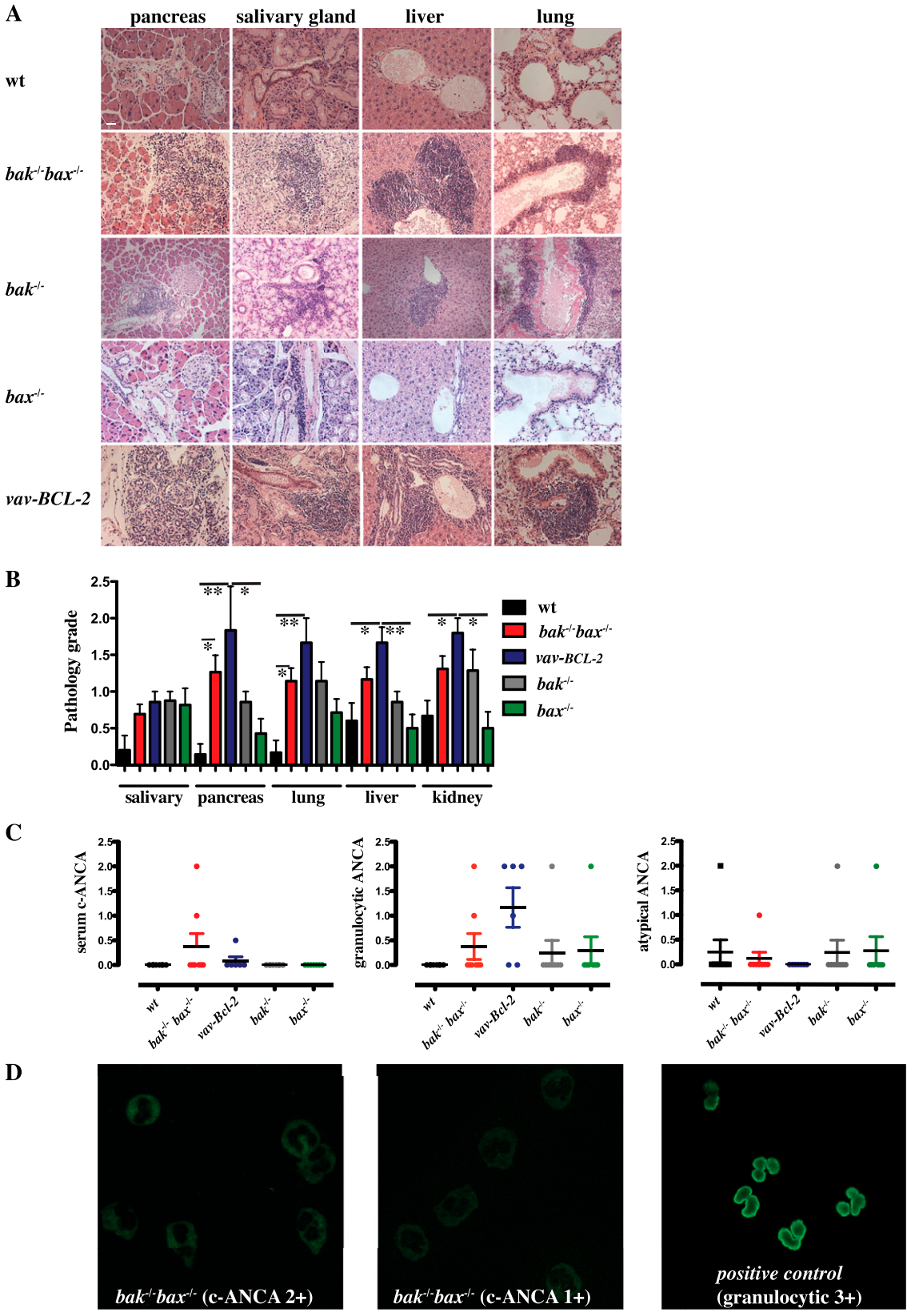

Fig. S6. Mice reconstituted with a $bak^{-/-}bax^{-/-}$, *vav-BCL-2*, or $bak^{-/-}$ hematopoietic system exhibit lymphocytic infiltrates in multiple organs. Representative photomicrographs (*A*) and summary (*B*) of the incidence of lymphocytic infiltration of the indicated tissues from mice reconstituted with a hematopoietic system of the indicated genotypes (n, number of mice analyzed per reconstitution genotype). Images of sections from the indicated tissues of Ly5.1 mice reconstituted with WT (238 d), $bak^{-/-}bax^{-/-}$ (104 d), $bak^{-/-}$ (240 d), $bax^{-/-}$ (322 d), or *vav-BCL-2* FLC (234 d). (Magnification: 20×; scale bar: 128 μm.) (*C*) Incidence of ANCA (c-ANCA, p-ANCA, and atypical ANCA) depicted graphically scored on a scale of 0–4, with six to eight mice analyzed for each genotype of hematopoietic reconstitution. (*D*) Representative photomicrographs of ANCA staining from Ly5.1 mice reconstituted with a hematopoietic system of the indicated genotypes.

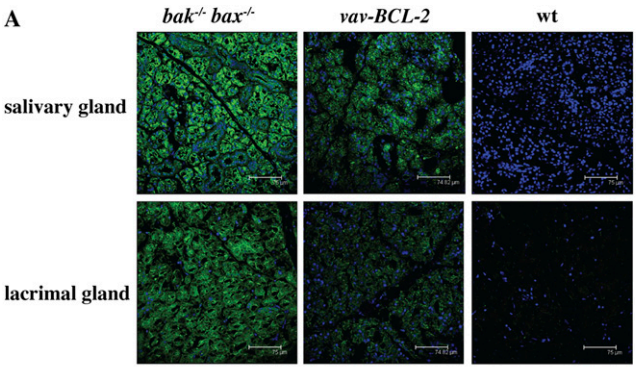

B

organ specific auto-antibodies (8 weeks)

donor	liver	salivary glands	lung	lacrimal gland	pancreas	n
bax$^{-/-}$ *bak*$^{-/-}$	0	38	0	75	0	8
vav-bcl-2	75	100	63	63	38	8
wt	0	0	0	0	0	8

Fig. S7. Tissue-specific autoantibodies are present 8 wk after hematopoietic reconstitution with *bak*$^{-/-}$*bax*$^{-/-}$ FLC. (*A*) Representative photomicrographs of immunofluorescence staining of frozen sections of salivary glands and lacrimal glands from a *rag-1*$^{-/-}$ mouse (to avoid the presence of endogenous immunoglobulins) stained with sera from Ly5.1 mice collected 8 wk after reconstitution with *bak*$^{-/-}$*bax*$^{-/-}$, *vav-BCL-2*, or WT FLC. (Scale bar: 75 μm.) (*B*) Summary of the incidence of organ-specific autoantibodies in Ly5.1 mice reconstituted with *bak*$^{-/-}$*bax*$^{-/-}$, *vav-BCL-2*, or WT FLC killed at 8 wk after reconstitution ($n = 8$/genotype). Numbers indicate percentages of mice with organ-specific autoantibodies ($n = 8$ for each genotype).

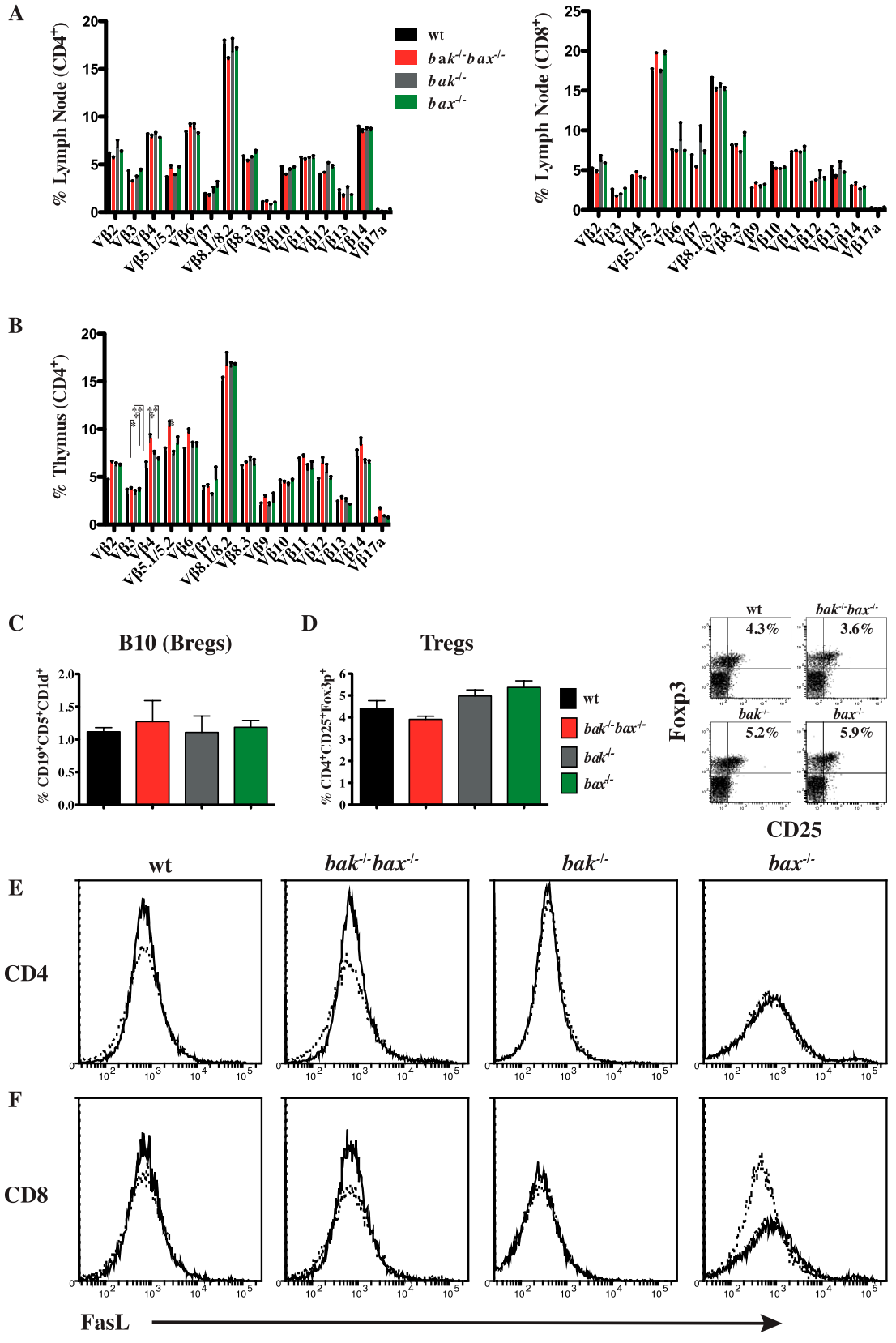

Fig. S8. T cell receptor (TCR) repertoire, content of B regulatory cells as well as T regulatory cells, and FasL expression on T cells in mice reconstituted with a *bak*$^{-/-}$*bax*$^{-/-}$ hematopoietic system. (*A*) Lymph node and (*B*) thymic CD4$^+$ T cells from mice reconstituted with a hematopoietic system of the indicated genotypes were analyzed for TCR Vβ use by flow cytometry. Data show the mean ± SEM of three mice per genotype. (*C*) The percentages of B10 B regulatory cells (CD19$^+$CD5$^+$CD1d$^+$) were detected by flow cytometric analysis in the lymph nodes of mice reconstituted with a hematopoietic system of the indicated genotypes (n = 3/genotype). (*D*) The percentages of T regulatory cells (CD4$^+$CD24$^+$Fox3p$^+$) were detected by flow cytometric analysis in the lymph nodes of

Legend continued on following page

mice reconstituted with a hematopoietic system of the indicated genotypes (n = 3/genotype). Representative flow cytometric plots gated on $CD4^+$ T cells are also shown (*$P < 0.05$; **$P < 0.005$). (*E*) Representative FACS histograms documenting the expression of surface FasL, as measured by flow cytometric analysis, on lymph node $CD4^+$ (*E*) or $CD8^+$ T (*F*) cells from mice reconstituted with a hematopoietic system of the indicated genotypes (solid line). Staining with an Ig isotype matched antibody (dotted line) is shown as a control (n = 3/genotype).

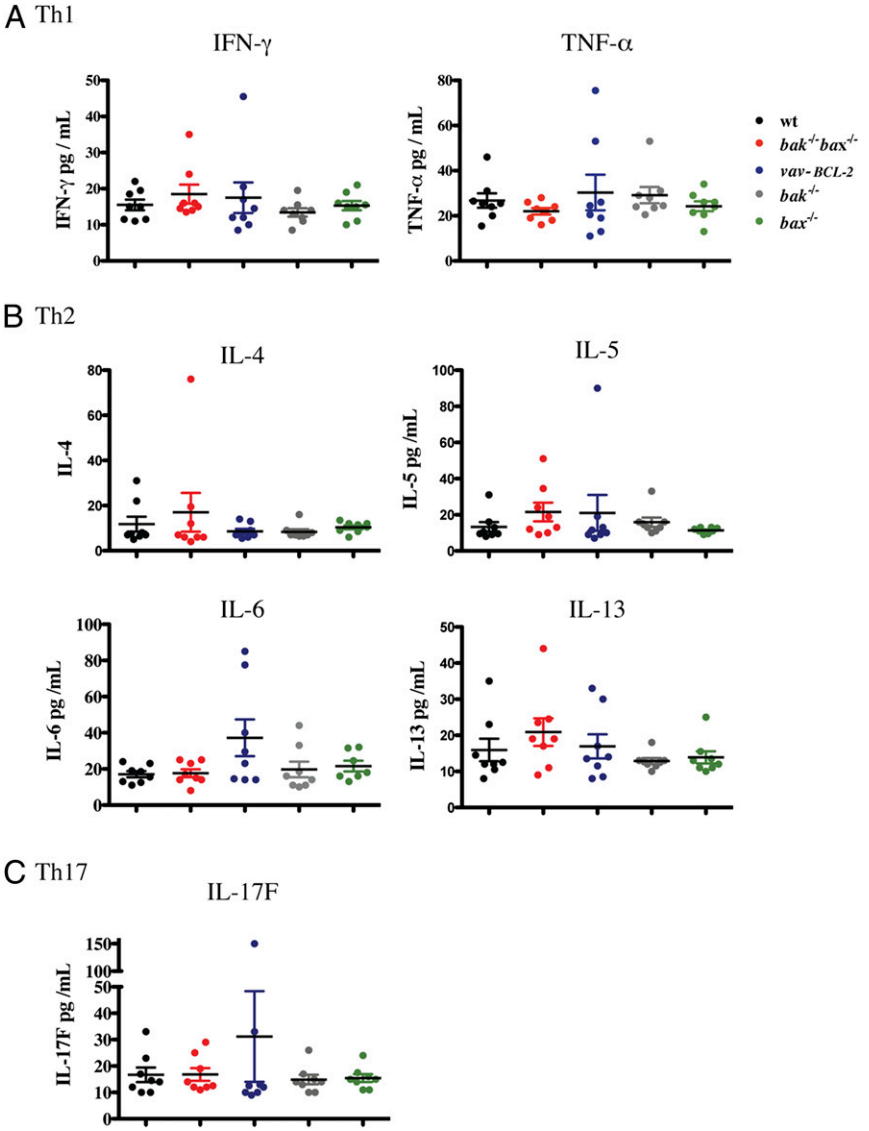

Fig. S9. Mice reconstituted with a $bak^{-/-}bax^{-/-}$ hematopoietic system do not have abnormal levels of cytokines or chemokines in their sera. Cytokines and chemokines (total of 23, determined by Bio-Rad Multiplex) were measured in the sera of sick mice that had been reconstituted with a $bak^{-/-}bax^{-/-}$ or $bak^{-/-}$ hematopoietic system or age-matched mice reconstituted with a WT or $bax^{-/-}$ hematopoietic system; n = 8/genotype. (*A*) Cytokines associated with a Th1 T-cell phenotype IFN-γ and TNF-α. (*B*) Cytokines associated with a Th2 T-cell phenotype, IL-4, -5, -6, and -13. (*C*) IL-17F expression levels associated with a Th17 T-cell phenoype. Data represent mean ± SEM.

Table S1. Summary of the incidence of organ-specific necrotizing vasculitis in mice reconstituted with a hematopoietic system of the indicated genotypes

Donor	Salivary glands	Pancreas	Spleen	Thymus	Kidney
bax$^{-/-}$*bak*$^{-/-}$	8 (13)	27 (15)	14 (14)	0 (12)	8 (39)
vav-bcl-2	14 (7)	67 (6)	50 (6)	25 (4)	23 (13)
bak$^{-/-}$	25 (8)	0 (7)	12 (8)	0 (6)	10 (21)
bax$^{-/-}$	0 (6)	0 (6)	ND	0 (6)	0 (6)
wt	0 (5)	0 (6)	0 (6)	0 (6)	0 (6)

Values are percentage of organs with vasculitis (number of mice analyzed per organ).

Table S2. Summary of presence (+) or absence (–) of organ-specific autoantibodies in mice reconstituted with a hematopoietic system of the indicated genotypes

Donor	Salivary glands	Thyroid	Pancreas	Stomach	Lacrimal	Retina
bax$^{-/-}$*bak*$^{-/-}$	+	–	+	+	+	+/–
vav-bcl-2	+	+	+	++	+	+
bak$^{-/-}$	+/–	+	+	+	+	+/–
bax$^{-/-}$	–	–	–	+	–	–
wt	–	–	–	–	–	–

++, strongly positive; +, moderately positive; +/–, trace; –, absence.